Available online at www.sciencedirect.com
ScienceDirect
IFAC PapersOnLine 56-2 (2023) 8237–8241

Effects of Velocity Profile and Plate Usage on Identified Bone Strength during Instrumented Screw Insertion ⋆

Jack Wilkie * **Ashish Bhave** ** **Georg Rauter** *** **Knut Möller** ****

* *Institute for Technical Medicine, Hochschule Furtwangen, Villingen-Schwenningen, Germany, (e-mail: wij@hs-furtwangen.de).*
** *Institute for Technical Medicine, Hochschule Furtwangen, Villingen-Schwenningen, Germany, (e-mail: bha@hs-furtwangen.de).*
*** *BIROMED-Lab, Department of Biomedical Egineering, University of Basel, Basel, Switzerland, (e-mail: georg.rauter@unibas.ch).*
**** *Institute for Technical Medicine, Hochschule Furtwangen, Villingen-Schwenningen, Germany, (e-mail: moe@hs-furtwangen.de).*

Abstract: Bone screws are important in orthopaedic surgery to treat fractures and secure implants. Over- or under-tightening these screws may lead to premature failure of the screw fixation, necessitating risky and costly revision surgery. Previously, a model-based method for automatically optimising bone screw insertion torque was developed. This paper expands on the prior testing of this method, to investigate how non-ideal conditions may affect the model accuracy/precision.
A bone screw was inserted into pre-drilled holes in artificial bone made from PU foam. Three cases were tested: first the screw was inserted directly with a constant velocity, then it was inserted with a trapezoidal velocity profile, and lastly it was inserted with a constant velocity profile, but through a hole in a metal plate. Each case was repeated 20 times for 60 total insertions. Torque and angular displacement measurements were used with a previously-developed model to identify the foam material strength for each insertion. Summary statistics were calculated for each case and statistical tests were used to compare the means and variances for the identified values between each case.
Comparing to base base case with constant velocity and no plate: we found a statistically significant ($p < 0.05$) difference in the mean identified strength for the trapezoidal velocity and the case with the plate. We found a statistically significant difference in the variance for the trapezoidal velocity profile ($p < 0.05$), but not for case with the plate present ($p = 0.16$).
Future work should investigate these effects over a wider range of materials and screws.

Keywords: Modelling, Biomedical control, Orthopaedic surgery, Bone screws, Biomechanics

1. INTRODUCTION

Bone screws are used in various surgical procedures. Typically, these procedures either fix traumatic fractures to assist natural healing, or secure implants (e.g. an artificial hip). In either case, maximising fixation strength and longevity is key to achieve good patient outcomes and avoid complications or revision surgery.

The torque used for tightening these screws influence the strength and longevity of the connection. If overtightened, the screws can damage the threads in the bone, compromising strength (Feroz Dinah et al., 2011), while under-tightening may lead to screws loosening over time when exposed to everyday cyclic loading and shock (Evans et al., 1990). Both may lead to premature failure of the screw fixation, requiring revision surgery; hence, optimising insertion torque is of interest to avoid the associated costs and risks.

In current practice, surgeons generally tighten screws ad-hoc by hand, or sometimes use fixed mechanical torque limiters. While surgeons are trained professionals, this requires a degree of subjective judgment during tightening, or selection of the appropriate torque limit. Additionally, errors may be more frequent for less experienced surgeons, and other human factors like stress and fatigue could impair judgment. An automated system for determining and enforcing an appropriate torque limit may provide an objective alternative that is unaffected by experience, stress, or fatigue.

Previous work has proposed and developed a model-based system targetting this goal. The system consists of two main steps: first the angular displacement and torque is monitored during screw insertion, and parameter identification methods are used to fit a model of the

⋆ This work was partially supported by grants “CiD” and “Digitalisation in the OR” from BMBF (Project numbers 13FH5E02IA and 13FH5I05IA).

10.1016/j.ifacol.2023.10.1007

Table 1. Properties of the PU foam utilised as a bone substitute, compared to real bone. ρ = density; σ_{ucs} = ultimate compressive strength; σ_{uts} = ultimate tensile strength; and E = Young's modulus.

Material name	ρ(g\cm^3)	σ_{ucs}(MPa)	σ_{uts}(MPa)	E(MPa)
SikaBlock® M150 (Sika Deutschland GmbH, 2020)	0.16	1.6	-	65
Cancellous Bone (Cornu et al., 2000; Schoenfeld et al., 1974)(Femoral head)	0.61-0.88	0.15-21	-	345-1475
Cortical Bone (Wall et al., 1979; Schoenfeld et al., 1974)(Femoral shaft)	1.83-2.03	-	63-101	6900

insertion to the recorded data in real time to determine the bone strength (Wilkie et al., 2021c); then second, this strength can be used to calculate a torque limit based on the known geometry of the screw and hole (Wilkie et al., 2021a). The torque limit could then be enforced with either a torque indicator, or an electromechanical torque-limiter/clutch. Other research has also investigated empirical screw stripping predictions based on plateau torque (Reynolds et al., 2017), rate of torque change (Thomas et al., 2008), and acoustic emissions (Wright et al., 2020).

Previous work on this model-based method has covered model development (Wilkie et al., 2021c,a), and testing (Wilkie et al., 2021b,a) under controlled conditions. This paper is investigating how some non-ideal conditions affect the identification of bone strength to better understand how these may affect the method in a more practical application in the future. Specifically, this paper is investigating the difference between inserting with a constant velocity, compared to the start-stop turning typical of hand insertion, and also the effects on insertion when inserting against a plate compared to simply inserting the screw directly into a hole, as screws may be used either alone or with plates in clinical settings.

2. METHODS

2.1 Experimental Procedure

Bone screws were inserted into polyurethane test blocks. The bone screws were HB 6.5 screws according to the ISO 5805:1991 standard (International Organization for Standardization, 1991) with a threaded length of approximately 30 mm and a 10 mm unthreaded shank. The screws were inserted into SikaBlock M150 rigid polyurethane blocks (Sika Deutschland GmbH, 2020), which are used as an artificial simulator of real bone (Calvert et al., 2010); the properties are presented in Table 1. The blocks were prepared with pre-drilled through-holes using a 3.0 mm drill bit, however a value of 3.2 mm was used later for the hole size due to the expected wobbling of the drill in the soft PU foam; a different unused hole was for each insertion. The screws were inserted at a controlled velocity using the test rig pictured in Figure 1 (Wilkie and Möller, 2021); this used a closed loop stepper motor (34HS46-6004D-E100 and CL86T, OMC Corporation Limited) constrained on linear guide rails to insert the screws in a controlled and repeatable manner while measuring rotation and torque using a rotational torque sensor (NCTE-2300-5-1-AU-0-0, NCTE AG) and displacement using a draw-wire encoder (A40/D5.2501.2421.1000, Fritz Kübler GmbH); 20 N of axial force was provided by a 2kg weight.

The insertions were repeated 20 times each for 3 different cases (total of 60 insertions). Each insertion consisted

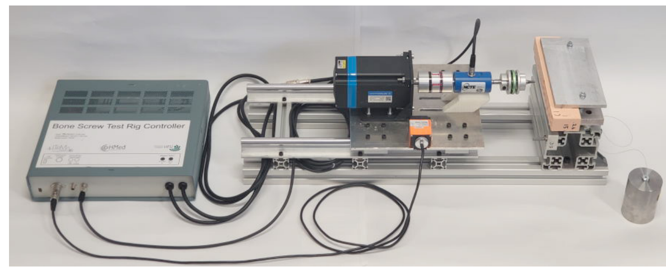

Fig. 1. Test rig used for screw insertion.

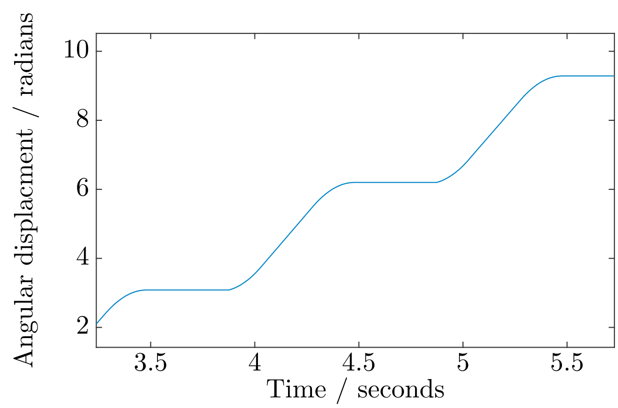

Fig. 2. Insertion profile recorded from screw insertion with trapezoidal angular velocity.

of 16 turns for the screw insertion, a 1s pause, then 17 turns for screw removal at a much faster speed. After approx. 13 turns the screw tightened and began to strip the threads until approx. 15 turns. Each insertion was zeroed at the point where the tip of the screw first entered the hole, by zeroing with an offset against a plate on known thickness placed atop the hole. In the first case, the screw was inserted at a fixed angular velocity of 30 RPM with nothing between the screw and the hole. In the second case, the screw was inserted at an average of 30 RPM with a trapezoidal velocity profile illustrated in Figure 2. In the third case, the screw was inserted at a constant velocity but a 1 mm thick plate was placed between the screw and the hole during insertion, as illustrated in Figure 3; this plate was left hanging on the screw during the insertion. During the insertion, data was logged at 1000 Hz, and prior to using the data below, the recordings were trimmed to the time period of screw insertion before tightening.

3. PARAMETER IDENTIFICATION

Each dataset was processed using a parameter identification technique to determine the strength of the hole material based on a simplified version of the model from Seneviratne et al. (2001). The parameter values are given and briefly described in Table 2. These parameters are used

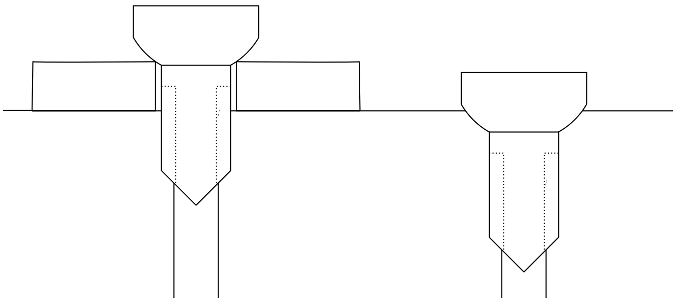

Fig. 3. Screw insertion diagram comparing insertion/tightening with and without a washer/plate.

Table 2. Values used in parameter identification.

Symbol	Value	Unit	Description
D_h	3.2	mm	Hole diameter
D_s	6.5	mm	Screw major diameter
2β	30	degrees	Screw thread angle
p	2.75	mm	Screw pitch
μ	0.14		Friction co-efficient
θ_t	60	degrees	Screw end taper

to calculate intermediary constants in Equations 1-5; r_f is the equivalent radius that frictional forces act through, r_s is the equivalent radius for cutting forces, A_c is the area of hole material that needs to be displaced for the screw to form a thread, θ is the thread helix angle at the edge, and K_{f0} relates screw geometry to frictional forces. These give 2 lumped geometric parameters in Equations 6 and 7 which relate to friction and cutting torque, respectively, which are combined in Equation 8 to give the overall torque as a function of angular displacement, ϕ.

$$r_f = (D_h + D_s)/4 \tag{1}$$

$$r_s = (2D_h + 2D_s)/6 \tag{2}$$

$$K_{f0} = \frac{1}{2}(D_s - D_h)\sqrt{(1 + tan^2\beta)\left[\left(\frac{D_s + D_h}{4}\right)^2 + \left(\frac{p}{2\pi}\right)^2\right]} \tag{3}$$

$$A_c = \tan\beta\left(\frac{D_s - D_h}{2}\right)^2 \tag{4}$$

$$\theta = \tan^{-1}\frac{p}{\pi D_s} \tag{5}$$

$$G_1 = r_s A_c \cos\theta \tag{6}$$

$$G_2 = 2r_f K_{f0}\cos\theta \tag{7}$$

$$\tau_z = \sigma_{ucs} G_1 + \mu\sigma_{ucs}\left(\phi - \frac{\alpha}{2}\right) G_2 \tag{8}$$

The σ_{ucs} value is the one unknown, representing the material strength of the bone, and is fitted with the least squares method in MATLAB R2020a based on measured torque data, τ_z, with the independent variable of angular displacement, ϕ.

3.1 Data Processing

The result from each test is an identified strength value, σ_{ucs}. This gave us 3 data sets of 20 values each for statistical analysis.

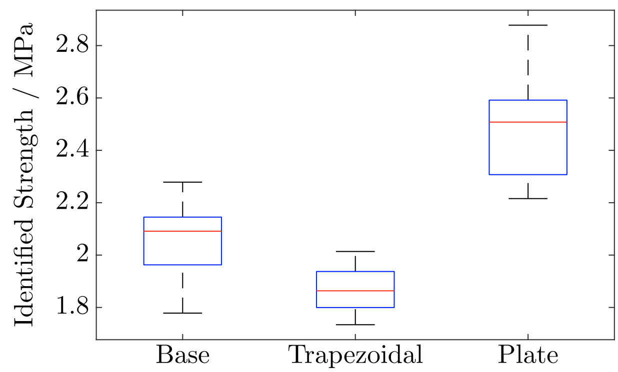

Fig. 4. Distributions of identified material strengths in the base case (constant velocity profile with no plate), compared to with a trapezoidal velocity profile or with a plate.

For each data set, summary statistics were made. The sample mean ($\bar{x}$) and standard deviations (s) were calculated, along with the standard errors ($SE(...)$) of these values according to the following equations (Rao et al., 1973)(n = sample size = 20):

$$SE(\bar{x}) = \frac{\sqrt{s^2}}{\sqrt{n}} \tag{9}$$

$$SE(s^2) = \frac{\sqrt{2s^4}}{\sqrt{n-1}} \tag{10}$$

$$SE(s) \approx SE(s^2)\frac{1}{2s} \tag{11}$$

To compare the means between the sets, the 2-sample t-test was performed in MATLAB R2020a with the ttest2() function to reject the null hypothesis of equal population means with $\alpha = 0.05$ (two-tail). To compare the variance, the 2-sample F-test was performed using the vartest2() function to reject the null hypothesis of equal population variance with $\alpha = 0.05$ (two tail). The test statistics and p-values were reported, as well as the 95% confidence interval for the variance ratios.

4. RESULTS

A box plot showing the distributions of identified values for each dataset is presented in Figure 4. The summary statistics for each distribution are presented in Table 3, and the statistical comparisons are presented in Table 4.

5. DISCUSSION

The mean identified strengths in each dataset in Table 3 ranged from 1.87 to 2.49 MPa, with the inter-dataset coefficient of variation (CoV) of the 3 sample means being 14.8%. Hence, by comparing to the CoV's within each dataset, the parameter identification inaccuracy error added by ignoring the differences between these datasets is approximately 2-3x higher than the "unavoidable" intra-dataset CoV of 4.6-7.7%. These values are also close to the data-sheet value of 1.6 MPa considering variation in the manufacturing and preparation of the PU foam test-blocks.

Table 3. Statistics for distributions of identification results. Values are for σ_{ucs} and are in MPa. SD = standard deviation, CoV (coefficient of variation) = SD/mean, SE = standard error.

Case	Mean	Mean SE	SD (CoV)	SD SE
No plate, constant velocity	2.07	0.031	0.139 (6.7%)	0.023
No plate, trapezoidal velocity	1.87	0.019	0.086 (4.6%)	0.014
Plate, constant velocity	2.49	0.043	0.192 (7.7%)	0.031

Table 4. Statistical test results comparing mean identified values (t-test) and variance (F-test) for the two non-idealities tested.

Comparison	t-test		F-test		
	t-statistic	p-value	F-statistic	p-value	Variance ratio 95% CI
Constant vs trapezoidal	5.50	3×10^{-6}	$F_{19,19} = 2.61$	0.04	$[1.03, 6.58]$
No plate vs plate	-7.88	2×10^{-9}	$F_{19,19} = 1.92$	0.16	$[0.21, 1.31]$

Comparing the base dataset (constant velocity insertion without plate) separately to the two others (trapezoidal velocity, or with the plate), both comparisons show a statistically significant ($p < 0.05$) difference in the sample means from the 2-sample t-tests in Table 4. It is worth noting that while the differences are statistically significant, it is not clear if they would be clinically significant as the sample mean from the trapezoidal case is only 10% less than the base case, and from the case with the plate it is only 20% more. Regardless, directly interpreting the statistical test suggests that these tested conditions affect the calibration of the model based method for determining the strength of bone, and to minimise errors, a practical application of this should have some way to identify and correct for the variation between these cases. The sample mean difference for the trapezoidal case may be due to the data sampling; while the sampling is at a constant rate w.r.t. time, the variable speed will give a varying rate w.r.t. displacement, weighting some displacement ranges more than others. This may add a slight bias to the fitted σ_{ucs}, resulting in the observed difference in sample means. For the case with the plate, the increase in average identified strength may arise from the plate adding a small amount of additional friction torque to the shaft of the screw during insertion, which is currently indistinguishable to the model from a harder bone material, as in Equation 8, torque is proportional to σ_{ucs}.

Table 4 also shows a statistically significant ($p < 0.05$) decrease in variance for the trapezoidal insertion profile compared to the base case, but no statistically significant difference with the plate present ($p = 0.16$). The decrease for trapezoidal insertion however, only just exceeds the threshold for the test, and the lower bound of the 95% confidence interval for the variance ratio is only 1.03, suggesting the difference may be very small. Again, interpreting the statistical test result directly, this suggests that different insertion velocity profiles may affect the precision of the model-based method for identifying bone strength, as the tighter variance in the trapezoidal case would translate to more consistent torque limit identification.

While this paper found some statistically significant differences between the datasets, and suggests further investigation is warranted, there are some limitations. Firstly, the variations may not be due to the different conditions, and could simply be due to variations/inhomogeneities in the material strength throughout the PU test blocks used for the insertions; this could include systematic variations in hole size arising from inconsistent drill runout. Secondly, this was only tested with a single type of screw in a single material; future work should test with a larger variety of bone screws and PU foam densities. Additionally, the PU foam does not perfectly imitate real bone, and the underlying physical/material-science causes for the results seen in PU foam may not match real bone; future testing should ideally also consider using real bone samples.

This paper investigated the effects of the non-ideal cases tested on the identified strength. A more comprehensive analysis should also consider the torque-limit model as part of the system, as, for example, the presence of a plate may change the torque capacity of the material.

6. CONCLUSION

We performed insertion tests of screws into artificial bone to test the effects of two non-ideal conditions on the identification of the bone strength with our previously-developed model-based method.

We found that changing from a constant angular velocity insertion to a varying trapezoidal profile caused a statistically significant ($p < 0.05$) change in the variance of the identified strengths (variance ratio 95% confidence interval $= [1.03, 6.58]$), and it caused a statistically significant ($p < 0.05$) 10% decrease in the mean identified strength.

Additionally, adding a plate for the screw to tighten against did not cause a statistically significant ($p = 0.16$) increase in the variance of the identified strengths, but still caused a statistically significant ($p < 0.05$) 20% increase in the mean identified strength.

Future work should expand on the screws and materials tested to test if these results apply in general, not just these specific conditions.

ACKNOWLEDGEMENTS

Thanks to Norbert Gut for providing workshop services for parts of the test rig setup and help preparing the test samples. Thanks to Andreas Dietz for providing the bone screws used for testing.

REFERENCES

Calvert, K.L., Trumble, K.P., Webster, T.J., and Kirkpatrick, L.A. (2010). Characterization of commercial rigid polyurethane foams used as bone analogs for implant testing. *J Mater Sci Mater Med*, 21(5), 1453–1461. doi:10.1007/s10856-010-4024-6.

Cornu, O., Banse, X., Docquier, P.L., Luyckx, S., and Delloye, C. (2000). Effect of freeze-drying and gamma irradiation on the mechanical properties of human cancellous bone. *Journal of Orthopaedic Research*, 18(3), 426–431. doi:10.1002/jor.1100180314.

Evans, M., Spencer, M., Wang, Q., White, S.H., and Cunningham, J.L. (1990). Design and testing of external fixator bone screws. *Journal of Biomedical Engineering*, 12(6), 457–462. doi:10.1016/0141-5425(90)90054-Q.

Feroz Dinah, A., Mears, S.C., Knight, T.A., Soin, S.P., Campbell, J.T., and Belkoff, S.M. (2011). Inadvertent Screw Stripping During Ankle Fracture Fixation in Elderly Bone. *Geriatr Orthop Surg Rehabil*, 2(3), 86–89. doi:10.1177/2151458511401352.

International Organization for Standardization (1991). ISO 5835:1991(en), Implants for surgery — Metal bone screws with hexagonal drive connection, spherical under-surface of head, asymmetrical thread — Dimensions. https://www.iso.org/obp/ui/#iso:std:iso:5835:ed-1:v1:en.

Rao, C.R., Rao, C.R., Statistiker, M., Rao, C.R., and Rao, C.R. (1973). *Linear Statistical Inference and Its Applications*, volume 2. Wiley New York.

Reynolds, K.J., Mohtar, A.A., Cleek, T.M., Ryan, M.K., and Hearn, T.C. (2017). Automated Bone Screw Tightening to Adaptive Levels of Stripping Torque. *Journal of Orthopaedic Trauma*, 31(6), 321–325. doi:10.1097/BOT.0000000000000824.

Schoenfeld, C.M., Lautenschlager, E.P., and Meyer, P.R. (1974). Mechanical properties of human cancellous bone in the femoral head. *Med. & biol. Engng.*, 12(3), 313–317. doi:10.1007/BF02477797.

Seneviratne, L.D., Ngemoh, F.A., Earles, S.W.E., and Althoefer, K.A. (2001). Theoretical modelling of the self-tapping screw fastening process. *Proceedings of the Institution of Mechanical Engineers, Part C: Journal of Mechanical Engineering Science*, 215(2), 135–154. doi:10.1243/0954406011520562.

Sika Deutschland GmbH (2020). SikaBlock M150 Product Data Sheet.

Thomas, R.L., Bouazza-Marouf, K., and Taylor, G.J.S. (2008). Automated surgical screwdriver: Automated screw placement. *Proc Inst Mech Eng H*, 222(5), 817–827. doi:10.1243/09544119JEIM375.

Wall, J.C., Chatterji, S.K., and Jeffery, J.W. (1979). Age-related changes in the density and tensile strength of human femoral cortical bone. *Calcif Tissue Int*, 27(1), 105–108. doi:10.1007/BF02441170.

Wilkie, J.A. and Möller, K. (2021). Test rig for bone screw insertion modelling. In *15th Interdisciplinary Symposium Automation in Medical Engineering (AUTOMED)*, 2. Basel, Switzerland. doi:10.5281/zenodo.4922937.

Wilkie, J., Docherty, P.D., and Möller, K. (2021a). Stripping Torque Model for Bone Screws. *IFAC-PapersOnLine*, 54(15), 442–447. doi:10.1016/j.ifacol.2021.10.296.

Wilkie, J., Docherty, P.D., Stieglitz, T., and Möller, K. (2021b). Quantifying Accuracy of Self-Tapping Screw Models. In *2021 43rd Annual International Conference of the IEEE Engineering in Medicine Biology Society (EMBC)*, 4391–4394. doi:10.1109/EMBC46164.2021.9630646.

Wilkie, J., Docherty, P.D., Stieglitz, T., and Moller, K. (2021c). Geometric Generalization of Self Tapping Screw Insertion Model. In *2021 43rd Annual International Conference of the IEEE Engineering in Medicine Biology Society (EMBC)*, 4. doi:10.1109/EMBC46164.2021.9630157.

Wright, B.J., Grigg, S., Bergsaker, A.S., Brattgjerd, J.E., Steen, H., and Pullin, R. (2020). Real time monitoring of screw insertion using acoustic emission can predict screw stripping in human cancellous bone. *Clinical Biomechanics*, 76, 105026. doi:10.1016/j.clinbiomech.2020.105026.